

# DPFNet: A Dual-branch Dilated Network with Phase-aware Fourier Convolution for Low-light Image Enhancement

Yunliang Zhuang<sup>1</sup>, Zhuoran Zheng<sup>2</sup>, Yuang Zhang<sup>1</sup>, Lei Lyu<sup>1</sup>, and Chen Lyu<sup>1</sup>

<sup>1</sup> School of Information Science and Engineering, Shandong Normal University,  
Jinan, 250014, China

lvchen@sdsnu.edu.cn

<sup>2</sup> School of Computer Science and Engineering, Nanjing University of Science and  
Technology, Nanjing, 210014, China

**Abstract.** Low-light image enhancement is a classical computer vision problem aiming to recover normal-exposure images from low-light images. However, convolutional neural networks commonly used in this field are good at sampling low-frequency local structural features in the spatial domain, which leads to unclear texture details of the reconstructed images. To alleviate this problem, we propose a novel module using the Fourier coefficients, which can recover high-quality texture details under the constraint of semantics in the frequency phase and supplement the spatial domain. In addition, we design a simple and efficient module for the image spatial domain using dilated convolutions with different receptive fields to alleviate the loss of detail caused by frequent down-sampling. We integrate the above parts into an end-to-end dual branch network and design a novel loss committee and an adaptive fusion module to guide the network to flexibly combine spatial and frequency domain features to generate more pleasing visual effects. Finally, we evaluate the proposed network on public benchmarks. Extensive experimental results show that our method outperforms many existing state-of-the-art ones, showing outstanding performance and potential. We release our code at <https://github.com/Zhuangyunliang/DPFNet>.

**Keywords:** Low-light Image Enhancement · Phase-aware Fourier Convolution · Dilated Convolution

## 1 Introduction

Images as a modality with a large number of discrete units can convey a wealth of information. However, due to unavoidable environmental or technical limitations (such as inadequate lighting and limited exposure time), images taken in low-light conditions do not effectively convey real-world color and texture information. Meanwhile, low-light images pose challenges for high-level computer vision tasks such as semantic segmentation, object detection, and image classification [2, 11, 25]. Therefore, enhancing the luminance and texture of low-light images for high-level vision tasks is a non-trivial problem.

Currently, most researchers propose various methods that can effectively improve the subjective and objective quality of low-light images. Traditional low-light image enhancement methods [3,21,34] use nonlinear mapping of pixel values from low-light images to achieve enhanced images. However, the carefully chosen parameters and optimization process of this class of methods require much knowledge and experience from the user and cannot be generalized to real-world scenes. Recently, learning-based methods [27] have shown great potential and have received widespread attention for their better effectiveness, robustness, and generalizability than traditional methods. For instance, Lore et al. [15] first applied deep neural networks to low-light image enhancement tasks and proposed an algorithm based on an autoencoder structure. Liang et al. [12] proposed a transformer-based image restoration method.

Despite the significant performance improvements of deep learning-based methods, several significant challenges remain for low-light image enhancement tasks: **1)** The frequency domain information of the image helps to reconstruct high-frequency texture details, making up for the loss of information in the spatial domain [32]. However, due to the limitation of real-valued convolution kernels, existing work [24] usually omit or separately processes phase information, making the reconstruction process lack semantic guidance in phase. **2)** Most of the above methods use stacked convolution kernels and up/down sampling to learn the features of global and different receptive fields. However, such schemes tend to lead to loss of texture details, which can seriously affect the result of the reconstructed images [13]. **3)** Transformer-based method shows strong competitiveness, proving the effectiveness of long-term dependence on the low-level image processing tasks. However, due to the characteristics of the self-attention mechanism, such methods usually depend on expensive hardware resources and a large amount of data samples [28,36].

To alleviate the above challenges, we propose a dual-branch dilated Network with phase-aware Fourier convolutions, named DPFNet. DPFNet can enhance low-light images in the frequency and spatial domains, respectively. In particular, we design a phase-aware Fourier convolution module to provide additional information for spatial domain reconstruction by exploiting the frequency domain characteristics after the fast Fourier transform (FFT). The module achieves the perception of semantic information in the phase by sharing the weights of the memory to combine the magnitudes for better performance dynamically. Due to the characteristics of the FFT, it can cover the receptive field to the entire image space at an early stage and efficiently perceive the global difference between low-light and normal-exposure images. In addition, we adopt a dilated convolution module with multi-level receptive fields to perform the enhancement on the spatial domain. This module can reduce the loss of image detail information caused by successive downsampling and economize the computational effort. Finally, we introduce a fusion module to fuse the enhancement results from the spatial and frequency domains and design a Fourier loss added to the loss committee to balance the different domains. Extensive experiments demonstrate that our proposed DPFNet outperforms state-of-the-art methods on public datasets.

In summary, our main contributions are threefold:

- We design a phase-aware Fourier convolution module that reconstructs high-frequency texture details guided by phase semantic information in image Fourier space to complement the spatial domain.
- We integrate spatial and frequency domain enhancements into an end-to-end dual-branch network. The network is capable of integrating low- and high-frequency information while capturing local and global interactions.
- We propose a Fourier loss added to the loss committee to balance features in the spatial and frequency domains to restore natural images.

## 2 Related Work

### 2.1 Deep Low-light Image Enhancement

With incentives from the good results of deep learning in various tasks, many researchers have started investigating low-light image enhancement algorithms [13,29,31] based on deep learning. Lore et al. [15] proposed an autoencoder deep learning network for low-light image enhancement. Zhang et al. [38] developed three sub-networks for layer decomposition, reflection recovery, and illumination adjustment, called KinD. Wang et al. [27] used a normalized flow model to establish a mapping between low-light and normal-light images. This allows for determining the correct conditional distribution of the enhanced images. However, these methods focus only on the spatial domain when enhancing low-light images and ignore information in the frequency domain. We propose a PFM that acts in the image frequency domain to recover the high-frequency texture details of normally-exposed images. In addition, such methods often use continuous downsampling to obtain large fields of perception, which leads to a loss of detailed information. We use dilated convolutions with different dilation rates to obtain information from different receptive fields, thereby mitigating the downsampling damage.

### 2.2 Applications of Fourier Transform

In recent years, the Fourier domain of images is often applied to accomplish different tasks with favorable results, which provides a new perspective for computer vision tasks based on images. Rao et al. [20] proposed that GFNet learns spatial long-term dependencies from the frequency domain and shows power competitiveness in image classification tasks. Mao et al. [17] designed a plug-and-play Fourier module to enhance the details of the deblurring algorithm. Wang et al. [24] designed a fast Fourier convolution to improve the perceptual quality and parameter efficiency of mask inpainting networks. However, most methods directly use the amplitude component of the Fourier coefficients or simply relate phase and amplitude, ignoring the semantic guidance of phase. Thus, we carefully design the Fourier convolution module to strengthen the connection between the two through associative memory with conjugate symmetry constraint on the spectral-domain weights.

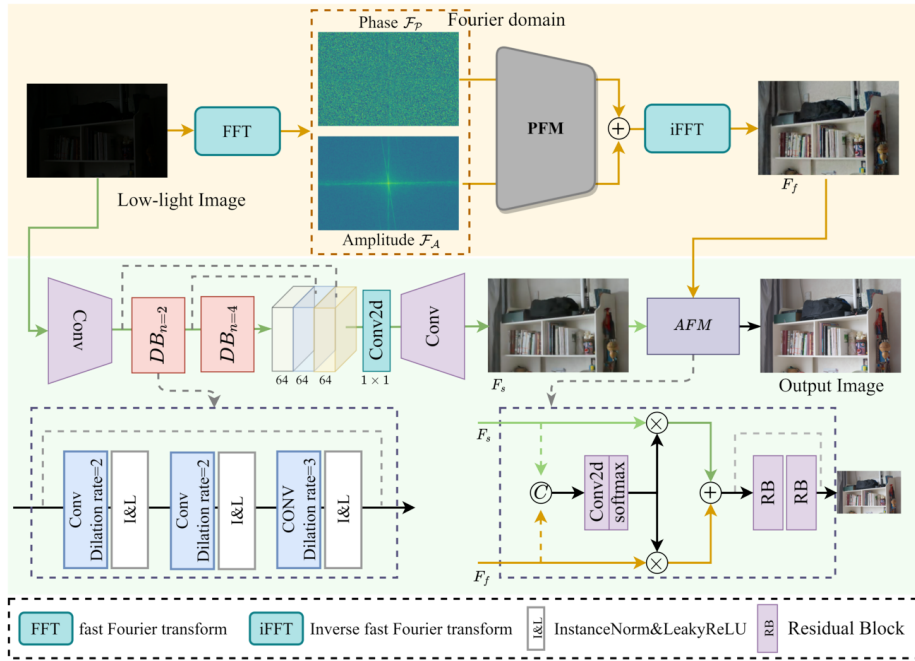


Fig. 1. The overall architecture of our proposed DPFNet.

### 3 Methodology

This section describes our proposed DPFNet. Inspired by [9, 35], we adopt a network structure with two independent branches to avoid the noise introduced by the mutual interference between the spatial and frequency domains during processing. DPFNet is mainly composed of two feature enhancement streams and a feature fusion. As shown in Figure 1, given the low-light images  $I_{low}$  as input, our network uses the phase-aware Fourier convolution module (PFM) to generate feature maps in the Fourier domain that contain more global and high-frequency details (upper stream). Then, the multi-level dilated convolution module (MDCM) aggregates the local contextual and content features under different receptive fields in the spatial domain (bottom stream). Finally, the adaptive fusion module (AFM) fuses the spatial and frequency domain features to avoid over-enhancement artifacts and reconstruct more natural, high-quality images. We describe the design of each part of DPFNet in detail below.

#### 3.1 Phase-aware Fourier Convolution Module

The PFM aims to restore the high-frequency texture details with the assistance of frequency domain information to supplement the spatial domain. The input low-light image  $I_{low}$  is converted into the frequency domain by the FFT. It can

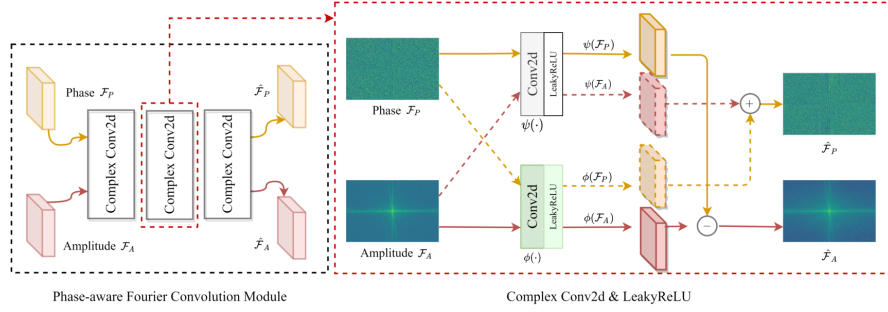


**Fig. 2.** The structure of our proposed Phase-aware Fourier Convolution Module.

be expressed as follows:

$$\mathcal{F}(u, v) = \sum_{x, y} I_{low}(x, y) e^{-j2\pi(\frac{u}{M}x + \frac{v}{N}y)}, \quad (1)$$

where  $I_{low}(x, y)$  and  $\mathcal{F}(u, v)$  are the spatial coordinates of the pixel and spectrum of the frequency domain, the height and width of the images are denoted  $(M, N)$ . Obviously, the spectrum of arbitrary frequency contains the global information under the spatial position.

We decompose the complex-valued form of the spectrum into the amplitude  $\mathcal{F}_A$  that contains the color texture and the phase  $\mathcal{F}_P$  that contains the semantic structure, and feed them into the PFM. To reduce the computational cost, we stack only three blocks with the same structure in the PFM, as shown in Figure 2. The block contains three complex convolutions with the kernel being  $3 \times 3$  and the LeakyReLU activation function. The complex convolution can enhance the phase semantic guidance [5], which is achieved by two different real-valued convolution operations, where the parameters of the filters of the real-valued convolution are shared. The operation process is formulated as:

$$\begin{aligned} \mathcal{F}_P &\leftarrow \phi(\mathcal{F}_P) + \psi(\mathcal{F}_A) \\ \mathcal{F}_A &\leftarrow \phi(\mathcal{F}_A) - \psi(\mathcal{F}_P), \end{aligned} \quad (2)$$

where the  $\phi(\cdot)$  and  $\psi(\cdot)$  are two uncorrelated convolutions. We finally use the inverse fast Fourier transform (iFFT) to reconstruct the enhanced spectrum of the frequency into spatial domain  $F_f$ , as follows:

$$F_f = iFFT(\mathcal{F}_A + j\mathcal{F}_P), \quad (3)$$

where  $j$  is the unit of the complex-valued imaginary part.

### 3.2 Multi-level Dilated Convolution Module

This section gives more details about this MDCM with dilated convolution blocks (DB). As shown in Figure 1, the low-light image  $I_{low}$  obtains the feature  $F_{local}$

of the local receptive field through 3-layer convolutional neural networks. Then,  $F_{local}$  is sequentially fed into multiple DBs, and multi-level features under a specific receptive field are obtained. We stack features of different receptive fields in the channel dimension ( $cat$ ) and aggregate them through non-overlapped convolutional layers with the kernel size being  $1 \times 1$ . This process is formulated as:

$$F_s = \phi(cat[DB_n(DB_{n-2}(F_{local})), DB_{n-2}(F_{local}), F_{local}]) \oplus F_{low}, \quad (4)$$

where  $n$  represents the dilation rate of the dilated convolution in DB. Inspired by [14], we add a convolution with the dilation rate =  $n + 1$  into each DB to alleviate grid artifacts.

### 3.3 Adaptive Fusion Module

To blend effectively the reconstructed high-quality features to preserve the regions with good visibility, we concatenate the extracted features  $F_f$  of the frequency stream and the features  $F_s$  of the spatial stream in the channel dimension and feed them to a convolutional layer to learn two importance indexes  $w_f, w_s$ , which can be expressed as:

$$w_f, w_s = softmax(Conv(cat[F_f, F_s])), \quad (5)$$

where  $Conv(\cdot)$  is the convolution layer with two kernels being  $3 \times 3$ . In the importance indexes, each pixel is assigned a corresponding weight, which is multiplied by the corresponding feature element by element to reconstruct the outputs. The recovery process can be defined as follows:

$$I_{norm} = RB_{\times 2}(F_f \otimes w_f \oplus F_s \otimes w_s), \quad (6)$$

where the  $\otimes$  denoted element multiplication and the  $\oplus$  represents element addition. Note that the outputs are passed through two residual blocks (RB) to generate the final result  $I_{norm}$  to capture subtle changes in image enhancement so that the enhanced image appears natural.

### 3.4 Loss Function

We adopted a loss committee consisting of three parts, each with specific capabilities.

**SSIM Loss.** Since the degradation of low-light images is related to many different factors, using  $l_1$  or  $l_2$  as the loss function leads to different degrees of distortion and does not give the most desirable results. In contrast, we adopt the SSIM loss to integrally evaluate differences such as luminance, contrast, and structure. Specifically, the  $\mathcal{L}_s$  is defined as:

$$\mathcal{L}_s = 1 - SSIM(I_{norm}, I_{gt}), \quad (7)$$

where  $I_{norm}, I_{gt}$  represent enhanced images and ground truth, and  $SSIM(\cdot)$  denotes the SSIM [39] operator.

**Fourier Loss.** To improve the sensitivity of our proposed model to frequency feature, we propose a Fourier Loss ( $\mathcal{L}_f$ ) based on frequency domain space to guide the model to reconstruct high-frequency detail. The  $\mathcal{L}_f$  can be considered as a weighted average of the frequency distance between the ground truth and the enhanced image, which is

$$\mathcal{L}_f = \frac{1}{N} \sum_{i=0}^N \|\text{cat}[I_{gt}^A, I_{gt}^P] - \text{cat}[I_{norm}^A, I_{norm}^P]\|^2 \quad (8)$$

where  $I_{gt}^A, I_{gt}^P$  represents the amplitude and phase components of the ground truth images by the FFT transform, which are concatenated together in the channel dimension, jointly minimizing the gap between the ground truth and the enhanced image.

**Perceptual Loss.** We introduce Perceptual loss ( $\mathcal{L}_p$ ) [8] as a perceptual measure to exploit image semantic information and improve the visual quality of enhanced images. Specifically, we use Euclidean distance to calculate the difference between feature maps, and the formula is defined as follows:

$$\mathcal{L}_p = \frac{1}{WHC} \|\phi(I_{gt}) - \phi(I_{norm})\|^2, \quad (9)$$

where  $W, H$  and  $C$  denote the three dimensions of the image, respectively, and the pre-trained VGG network [23] is denoted as  $\phi(\cdot)$ .  $\mathcal{L}_p$  balances the guiding role of  $\mathcal{L}_s$  and  $\mathcal{L}_f$ , ensuring the stability of our network training process.

**Total Loss.** We use the loss committee to construct the total loss function, which is

$$\mathcal{L} = \mathcal{L}_s + \lambda_a \mathcal{L}_f + \lambda_b \mathcal{L}_p, \quad (10)$$

where  $\lambda_a$  and  $\lambda_b$  are trade-off weight hyperparameters. Extensive experiments demonstrate that the best results of our network are obtained when  $\lambda_a = 1.0$  and  $\lambda_b = 0.2$ .

## 4 Experiments

We validate our model on two datasets, including the LOL [6] and the MIT-5K [1] datasets. LOL dataset contains 500 pairs of images taken by real cameras. We selected 485 pairs as the training set and 15 pairs as the test set. MIT-5K dataset contains 5000 images taken with a DSLR camera. Similar to [1, 6, 26], we used the results of the expert C adjustment for ground-truth and used the first 4500 images for training and the last 500 for testing.

The implementation of the environment uses the PyTorch [19] framework, trained and tested on Intel(R) Xeon(R) Gold 5218 CPU @ 2.30GHz, 128G RAM, and TITAN RTX GPU (24G RAM) platform. We set the batch size to 4 and trained our model using the Adam optimizer with  $\beta_1 = 0.9$ ,  $\beta_2 = 0.999$  and  $\epsilon = 10^{-8}$ . The learning rate is initialized to 0.0001, and 200 epochs are enforced, decaying by a factor of 0.5 in every 50 epochs. We randomly cropped the training images to  $256 \times 256$  and normalized the pixel values to the interval  $[0, 1]$  as the input to the network.



**Fig. 3.** Visual comparisons with state-of-the-art low-light image enhancement methods on the LOL and MIT-5K datasets.

#### 4.1 Performance Comparison

**Quantitative Evaluation.** Our proposed method is compared with ten low-light image enhancement methods [3, 10, 13, 16, 21, 27, 30, 33, 34, 37] on the LOL and MIT-5K datasets, and the results are shown in Table 1. Among them, the results of SSIM [4], PSNR [7], and NIQE [18] are the average values of the corresponding test sets, and the **bolded data** indicate the best results for that test set. As can be seen from Table 1, our method can achieve better performance compared to other low-light image enhancement methods. On the LOL dataset, our method achieves 1.23dB improvement in PSNR and 0.012dB in SSIM compared to the previous LLFlow method. Furthermore, our method also significantly outperforms other methods on the MIT-5K dataset.

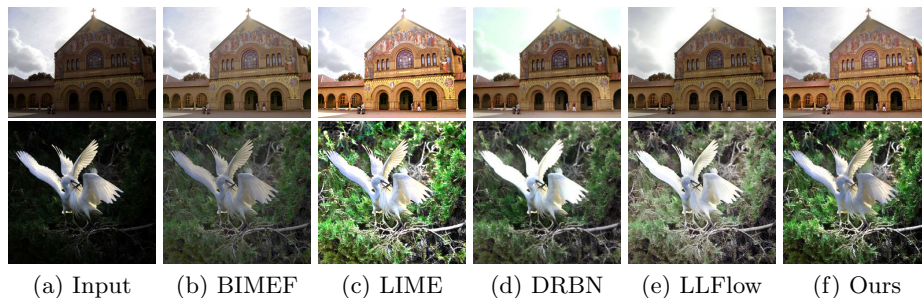
**Qualitative Evaluation.** In order to compare the effect of enhanced images more intuitively, we selected random images from the datasets and visualized



**Table 1.** Compare quantization with the state-of-the-art image enhancement methods in LOL and MIT-5K datasets.

	BIMEF	CRM	LIME	RetinexNet	MBLLEN	DSLR	DRBN	ZeroDCE++	KinD++	LLFlow	Ours
PSNR↑	13.88	17.20	16.76	16.77	17.56	18.24	20.13	19.43	21.30	22.92	<b>24.15</b>
LOL SSIM↑	0.577	0.644	0.564	0.567	0.736	0.787	0.802	0.768	0.822	0.837	<b>0.849</b>
NIQE↓	7.69	8.02	9.13	9.73	<b>3.46</b>	4.11	4.63	7.79	5.11	4.03	3.94
PSNR↑	18.67	13.99	11.21	20.81	16.42	17.02	20.95	16.46	22.01	25.03	<b>25.33</b>
MIT5K SSIM↑	0.693	0.674	0.667	0.687	0.851	0.750	0.794	0.766	0.832	8.521	<b>0.910</b>
NIQE↓	3.87	4.22	4.50	4.48	4.19	3.90	5.44	3.92	4.15	3.49	<b>3.42</b>

them using the method described above. According to Figure 3, we can clearly observe that the enhanced images by the traditional physics-based methods (such as BIME, CRM, and LIME) are still insufficient and generate amplified noise. The images produced by KinD++, LLFlow, and other deep learning-based approaches still have a large number of artifacts at the edges. In contrast, our method enabling it to significantly enhance different degrees of darkness, and the enhanced images have more texture detail and better visual experience. In order to demonstrate the generalization ability of our network in real scenes, we selected some classical algorithms to compare the effect of enhancing real low-light images. As shown in Figure 4, our method can equally effectively improve the real-world image of the darkness problem with an exciting performance.

**Fig. 4.** Visual comparisons with state-of-the-art low-light image enhancement methods on the no-reference datasets. (a) is the original input image, and (b)-(f) represent the images enhanced by SOTA and our method, respectively.

## 4.2 Ablation Study

**Effectiveness of Network Architecture.** We established MDCM as baseline and compared it with the classic U-Net [22]. Then, we sequentially add PFM (denoted MDCM w/ PFM) and AFM (DPFNet) to demonstrate the effectiveness of our proposed module. As shown in Table 2, our proposed MDCM improves

**Table 2.** Quantified results of ablation experiments for network components.

Datasets	U-Net		MDCM		MDCM w/ PFM		DPFNet	
	PSNR	SSIM	PSNR	SSIM	PSNR	SSIM	PSNR	SSIM
LOL	18.13	0.796	21.16	0.813	23.67	0.835	24.15	0.849
MIT5K	20.47	0.825	23.92	0.851	24.84	0.874	25.33	0.910

the PSNR by 3.03dB compared with UNet of frequently downsampled. With the addition of PFM, our model improves PSNR by 2.51 dB on the LOL dataset and 0.92 dB on the MIT-5K dataset. This also validates the importance of fusing frequency domain information with the help of PFM to enhance the enhancement effect of dark images. In addition, the AFM helps our network balance frequency and spatial domain features, increasing PSNR by 0.48 dB on the LOL dataset and by 0.49 dB on the MIT-5K dataset.

**Fig. 5.** Visual results of loss component in the loss committee on the LOL dataset.

**Effectiveness of Loss Function.** We use the SSIM loss ( $\mathcal{L}_s$ ) as the essential content loss, then the Fourier loss ( $\mathcal{L}_f$ ) and Perceptual loss ( $\mathcal{L}_p$ ) are added to guide the network training. Figure 5 shows the intuitive comparison results, we can observe that the SSIM loss has been able to make the model produce satisfactory results, but the details are still lacking. The addition of Fourier loss helps better PFM perceive high-frequency details, but the restored image has an over-enhanced effect. Finally, it can be seen that the Perceptual loss constrains the model-enhanced images at a high level of semantics, enabling our DPFNet to produce more natural images.

## 5 Conclusion

In this paper, we propose a novel low-light image enhancement network. For this network, we propose a Phase aware Fourier convolution module. The module can provide high-frequency information for spatial domain reconstruction by exploiting the properties of Fourier coefficients to generate sharper images. In addition, we design a dilated convolution module that aggregates features from different receptive fields to alleviate the loss caused by the downsampling of common network structures. We integrate the above parts into a two-branch framework to enhance spatial and frequency domain information. Finally, to reconstruct a more natural result, we propose a Fourier loss and adaptive fusion module to

guarantee the stability of network training. Quantitative and qualitative results show that our algorithm can recover sharper images and exhibit more potential.

## References

1. Bychkovsky, V., Paris, S., Chan, E., Durand, F.: Learning photographic global tonal adjustment with a database of input/output image pairs. In: CVPR 2011. pp. 97–104 (2011)
2. Gnanasambandam, A., Chan, S.H.: Image classification in the dark using quanta image sensors. In: ECCV. pp. 484–501 (2020)
3. Guo, X., Li, Y., Ling, H.: Lime: Low-light image enhancement via illumination map estimation. *IEEE Trans Image Process* **26**(2), 982–993 (2016)
4. Hore, A., Ziou, D.: Image quality metrics: Psnr vs. ssim. In: ICPR. pp. 2366–2369 (2010)
5. Hu, Y., Liu, Y., Lv, S., Xing, M., Zhang, S., Fu, Y., Wu, J., Zhang, B., Xie, L.: Dccrn: Deep complex convolution recurrent network for phase-aware speech enhancement. arXiv preprint arXiv:2008.00264 (2020)
6. Hu, Y., He, H., Xu, C., Wang, B., Lin, S.: Exposure: A white-box photo post-processing framework. *ACM Trans. Graph.* **37**(2), 1–17 (2018)
7. Huynh-Thu, Q., Ghanbari, M.: Scope of validity of psnr in image/video quality assessment. *Electron. Lett.* **44**(13), 800–801 (2008)
8. Johnson, J., Alahi, A., Fei-Fei, L.: Perceptual losses for real-time style transfer and super-resolution. In: European conference on computer vision. pp. 694–711 (2016)
9. Koh, J., Lee, J., Yoon, S.: Bnucd: A two-branched deep neural network for restoring images from under-display cameras. In: CVPR. pp. 1950–1959 (2022)
10. Li, C., Guo, C., Loy, C.C.: Learning to enhance low-light image via zero-reference deep curve estimation. arXiv preprint arXiv:2103.00860 (2021)
11. Li, G., Yang, Y., Qu, X., Cao, D., Li, K.: A deep learning based image enhancement approach for autonomous driving at night. *Knowl Based Syst* **213**, 106617 (2021)
12. Liang, J., Cao, J., Sun, G., Zhang, K., Van Gool, L., Timofte, R.: Swinir: Image restoration using swin transformer. In: Proceedings of the IEEE/CVF International Conference on Computer Vision. pp. 1833–1844 (2021)
13. Lim, S., Kim, W.: Dslr: Deep stacked laplacian restorer for low-light image enhancement. *IEEE Trans Multimedia* **23**, 4272–4284 (2020)
14. Liu, J., Li, C., Liang, F., Lin, C., Sun, M., Yan, J., Ouyang, W., Xu, D.: Inception convolution with efficient dilation search. In: CVPR. pp. 11486–11495 (2021)
15. Lore, K.G., Akintayo, A., Sarkar, S.: Llnet: A deep autoencoder approach to natural low-light image enhancement. *Pattern Recognit* **61**, 650–662 (2017)
16. Lv, F., Lu, F., Wu, J., Lim, C.: Mbllen: Low-light image/video enhancement using cnns. In: BMVC. vol. 220 (2018)
17. Mao, X., Liu, Y., Shen, W., Li, Q., Wang, Y.: Deep residual fourier transformation for single image deblurring. arXiv preprint arXiv:2111.11745 (2021)
18. Mittal, A., Fellow, IEEE, Soundararajan, R., Bovik, A.C.: Making a ‘completely blind’ image quality analyzer. *IEEE Signal Process. Lett.* **20**(3), 209–212 (2013)
19. Paszke, A., Gross, S., Massa, F., Lerer, A., Bradbury, J., Chanan, G., Killeen, T., Lin, Z., Gimelshein, N., Antiga, L., et al.: Pytorch: An imperative style, high-performance deep learning library. arXiv preprint arXiv:1912.01703 (2019)
20. Rao, Y., Zhao, W., Zhu, Z., Lu, J., Zhou, J.: Global filter networks for image classification. *Advances in Neural Information Processing Systems* **34**, 980–993 (2021)

21. Ren, Y., Ying, Z., Li, T.H., Li, G.: Lecarm: Low-light image enhancement using the camera response model. *IEEE Trans Circuits Syst Video Technol* **29**(4), 968–981 (2018)
22. Ronneberger, O., Fischer, P., Brox, T.: U-net: Convolutional networks for biomedical image segmentation. In: *MICCAI*. pp. 234–241 (2015)
23. Simonyan, K., Zisserman, A.: Very deep convolutional networks for large-scale image recognition. *arXiv preprint arXiv:1409.1556* (2014)
24. Suvorov, R., Logacheva, E., Mashikhin, A., Remizova, A., Ashukha, A., Silvestrov, A., Kong, N., Goka, H., Park, K., Lempitsky, V.: Resolution-robust large mask inpainting with fourier convolutions. In: *WACV*. pp. 2149–2159 (2022)
25. Wang, H., Chen, Y., Cai, Y., Chen, L., Li, Y., Sotelo, M.A., Li, Z.: Sfnnet-n: An improved sfnnet algorithm for semantic segmentation of low-light autonomous driving road scenes. *IEEE trans Intell Transp Syst* (2022)
26. Wang, R., Zhang, Q., Fu, C.W., Shen, X., Zheng, W.S., Jia, J.: Underexposed photo enhancement using deep illumination estimation. In: *Proceedings of the IEEE/CVF Conference on Computer Vision and Pattern Recognition*. pp. 6849–6857 (2019)
27. Wang, Y., Wan, R., Yang, W., Li, H., Chau, L.P., Kot, A.C.: Low-light image enhancement with normalizing flow. In: *AAAI* (2022)
28. Wang, Z., Cun, X., Bao, J., Zhou, W., Liu, J., Li, H.: Uformer: A general u-shaped transformer for image restoration. In: *CVPR*. pp. 17683–17693 (2022)
29. Wei, C., Wang, W., Yang, W., Liu, J.: Deep retinex decomposition for low-light enhancement. *arXiv preprint arXiv:1808.04560* (2018)
30. Wei, C., Wang, W., Yang, W., Liu, J.: Deep retinex decomposition for low-light enhancement. *arXiv preprint arXiv:1808.04560* (2018)
31. Wu, W., Weng, J., Zhang, P., Wang, X., Yang, W., Jiang, J.: Uretinex-net: Retinex-based deep unfolding network for low-light image enhancement. In: *CVPR*. pp. 5901–5910 (2022)
32. Xu, K., Qin, M., Sun, F., Wang, Y., Chen, Y.K., Ren, F.: Learning in the frequency domain. In: *CVPR*. pp. 1740–1749 (2020)
33. Yang, W., Wang, S., Fang, Y., Wang, Y., Liu, J.: Band representation-based semi-supervised low-light image enhancement: Bridging the gap between signal fidelity and perceptual quality. *IEEE Trans Image Process* **30**, 3461–3473 (2021)
34. Ying, Z., Li, G., Gao, W.: A bio-inspired multi-exposure fusion framework for low-light image enhancement. *arXiv preprint arXiv:1711.00591* (2017)
35. Yu, Y., Liu, H., Fu, M., Chen, J., Wang, X., Wang, K.: A two-branch neural network for non-homogeneous dehazing via ensemble learning. In: *CVPR*. pp. 193–202 (2021)
36. Zamir, S.W., Arora, A., Khan, S., Hayat, M., Khan, F.S., Yang, M.H.: Restormer: Efficient transformer for high-resolution image restoration. In: *CVPR*. pp. 5728–5739 (2022)
37. Zhang, Y., Guo, X., Ma, J., Liu, W., Zhang, J.: Beyond brightening low-light images. *Int J Comput Vis* **129**(4), 1013–1037 (2021)
38. Zhang, Y., Zhang, J., Guo, X.: Kindling the darkness: A practical low-light image enhancer. In: *ACM MM*. pp. 1632–1640 (2019)
39. Zhao, H., Gallo, O., Frosio, I., Kautz, J.: Loss functions for image restoration with neural networks. *IEEE Trans Comput Imaging* **3**(1), 47–57 (2016)